



Numerical Investigations of Using Pressure-Side Winglet on Aerodynamic Performance of Compressor cascade

M. Attalla¹, Mohamed A. Mohamed^{1,2}, Mahmoud A. Mahmoud¹

¹Department of Mechanical Engineering, Faculty of Engineering, South Valley University, Qena, Egypt.

²School of Engineering, University of South Wales, Pontypridd, CF23 1DL, UK

Abstract A numerical simulation has been carried out to investigate the influences of pressure side winglet on controlling tip clearance flow in a low speed axial compressor cascade. The use of Winglet on the pressure-side of a highly loaded compressor cascade is investigated as a way of passive tip-leakage control. Two tip clearance gaps of 1.0% and 1.5% of the blade chord length are used to investigate the effect of tip gap variation on the tip leakage flow over the winglet geometry. Spalart-Allmaras (S-A) model was used in study as RANS turbulence model. The simulation results for the baseline and controlled blades were compared to experimental data. The numerical results showed that the pressure-side winglet increased the blade loading near the tip so, the strength of tip leakage flow was increased and the aerodynamic performance of a typical compressor blade is deteriorated.

Keywords Pressure-Side Winglet; Compressor Cascade; Numerical Simulation

Introduction

In axial compressor, to allow the relative motion between rotor and the casing wall and prevent physical wear and tear, a tip clearance is necessary. The size of the tip gap is typically given as a percentage of the blade chord/height length and usually equals to the few percentages. The pressure difference between the pressure surface and the suction surface of the blade will drive the fluids in the pressure side/end wall corner to the suction side/end wall corner, passing through the clearance, which is called tip leakage flow. A tip clearance flow is created through the gap and tip leakage vortex is generated. The resulting tip-leakage flow field is three-dimensional and highly unsteady leading to deteriorated aerodynamic performance of the compressor. Therefore, this problem has received substantial attention in the past and numerous numerical and experimental investigations of tip-leakage flow phenomenon have been carried out. Most of the past studies were aimed at aerodynamics performance. The large gap clearance was found to be deleterious to the performance and stability of linear compressor, however the optimum behavior was documented at a smaller clearances [1]. Experimental measurements and numerical simulations in a linear compressor cascade were performed to investigate the tip leakage flow with a tip size similar to that in the real compressor [2]. The results showed that the strength of the tip-leakage flow vortices depends on the tip clearance size where high losses are generated near to the gap exit. Numerical solution of the three-dimensional Navier-Stokes equations were obtained to investigate the tip-clearance flow leakage in a linear compressor cascade using Baldwin-Lomax turbulence model [3]. It was shown that the numerical simulation results agree with the experimental data and the flow field structure in the clearance gap was demonstrated.

As the tip-leakage flow has a considerable impact on the aerodynamic performance, efficiency, stability, energy transfer and obtained pressure rise in the axial compressor, researchers are strongly motivated by the urgent



need of improving these parameters thereby reducing the deteriorated effects of the tip-clearance flow. In that sense, passive flow control techniques have been applied extensively to control the tip-leakage flow. Geometrical modification of the blade tip using winglets is approved as an effective passive control device for reducing the total pressure loss associated with the tip clearance leakage flow [4]. Studies showed that the tip winglet passive control has a remarkable impact on the aerodynamics performance and pressure loss reduction in axial flow turbo-machinery. A detailed experimental study was carried out by using winglets at the blade tip as passive control method to control the tip leakage flow and enhance the aerodynamics performance of highly loaded axial compressor blades [5]. The wind tunnel tests were carried out using axial compressor cascade equipped with winglets mounted on suction, pressure and both sides of blade at three tip gap sizes of 1.0%, 1.5% and 2.0% of blade chord length. The results indicated that the passive tip-leakage flow control using winglets improved the aerodynamics performance of the axial compressor and reduced the total pressure loss at the cascade exit plane. Furthermore, the suction-side winglet was recognized to perform well and reduce the total pressure loss compared to both pressure and combined side winglets. Numerical studies using NUMECA commercial CFD package, were also carried out to predict the effect of both pressure-side [6] and suction-side [7] winglets in controlling the tip-leakage flow in an axial compressor cascade, respectively. Moreover, the effects of winglet width, clearance size and variations of incidence angles were also investigated. The results provided enough information about the mechanism of how the suction/pressure-side winglet controls the tip-leakage flow and enhances the total pressure loss through cascade passage. In the present paper, a numerical study using ANSYS CFD solver is carried out to get numerical comparison of the baseline and controlled blades by pressure-side winglet with the experimental data available. Moreover, Spalart-Allmars(S-A) is used as RANS turbulence model. The study is performed at two values of tip clearance sizes of $\tau = 1.0\% c$, and $1.5\% c$, where “ τ ” is tip clearance size and “ c ” is the blade chord length. The numerical results of both the baseline blade (no winglet – NW) and controlled blade with pressure-side winglet - PW) compared well with the experimental data.

Cascade and Blade Geometry

In the present study, pressure-side tip-winglet is applied to an axial compressor cascade to passively control the tip-leakage flow losses. Figure 1 shows a detailed view of the computational domain with a linear compressor cascade. The cascade consists of five cantilevered GE rotor B section blades. The blade has rounded leading and trailing edges and its maximum thickness is located at 60% chord length

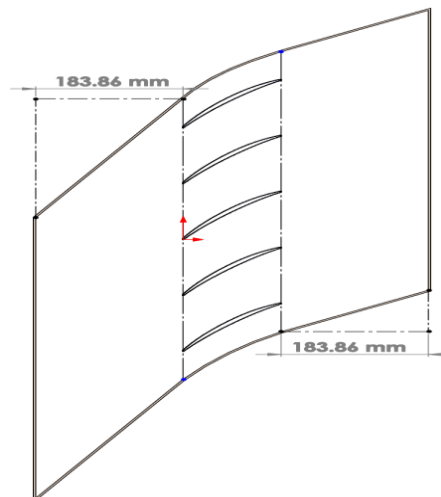


Figure 1: Computational domain with axial compressor cascade

The aerodynamic parameters of the compressor cascade are indicated in Table 1. The current study was used two different tip clearance (s) sizes in all simulation cases (baseline and pressure-side winglet) are set at 1.0% C , and 1.5% C .



Table 1: Cascade aerodynamic parameters

Parameter	Value
Stagger angle	50°
Chord (c)	160 mm
Axial chord (ca)	122.57 mm
Span (h)	160 mm
Pitch (p)	120 mm
Cascade inlet angle	35.8°
Camber angle	28.40°
Inlet flow angle	54.20°
Incidence	0.0°
Solidity	1.33

The winglet is a small tab that extends vertically from the blade suction surface. The winglet has width of 1.4 mm and it extends away from the blade surface by distance equals to 50% of the local blade tip thickness. The present numerical simulations are carried out using both baseline blades (NW) and controlled blades with tip-winglet as a passive flow control technique and added to pressure-side of blade as shown in Figure 2.

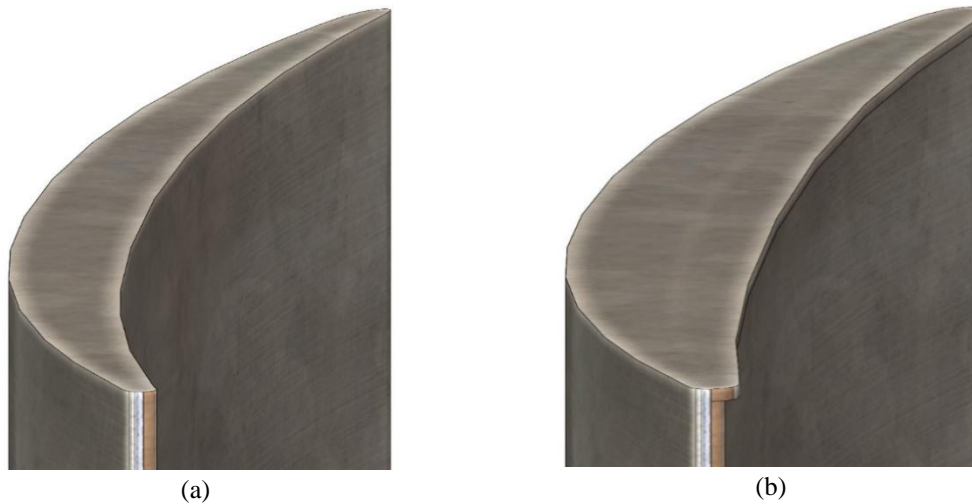


Figure 2: CAD model of the blade; (a) Baseline blade, (b) Pressure-side winglet

Computational Methods

A commercial CFD package is used in the present study to carry out all simulation phases, pre-processing, calculations and post-processing. A three-dimensional blade geometry, axial compressor cascade and computational domain are created using the DesignModeler software. The computational domain is extended upstream of the blade leading edge at the domain inlet by 1.5 times the axial chord and downstream of the blade trailing edge at the domain exit by the same distance. The computational domain around the cascade is divided into small blocks to control the grid generation in the regions close to the blade and tip-winglet. Structured boundary layer with hexahedron cells is created near the blades surfaces to model the wall shear stresses. A close-up view of the boundary layer close to blade leading and trailing edges and unstructured mesh for the whole computational domain are shown in Figures 3 (a) and (b), respectively.

The mesh was generated for the whole computational domain with high quality parameters for accurate simulation results. The aspect ratio was up to 175 and the orthogonal quality was kept at 0.025. Structured boundary layer cells were generated around each blade in the cascade with a resolution of 12 layers to ensure that the boundary layer was resolved. Moreover, the height of the centroid of the first cell from the blade surface was calculated to adjust the Y-Plus value to be in the range of $30 < Y+ < 100-300$. Unstructured mesh with



tetrahedron cells was generated for the rest of the computational domain. Figure 4 shows a close-up view of the unstructured mesh near the compressor blade with pressure side tip-winglet (PW)

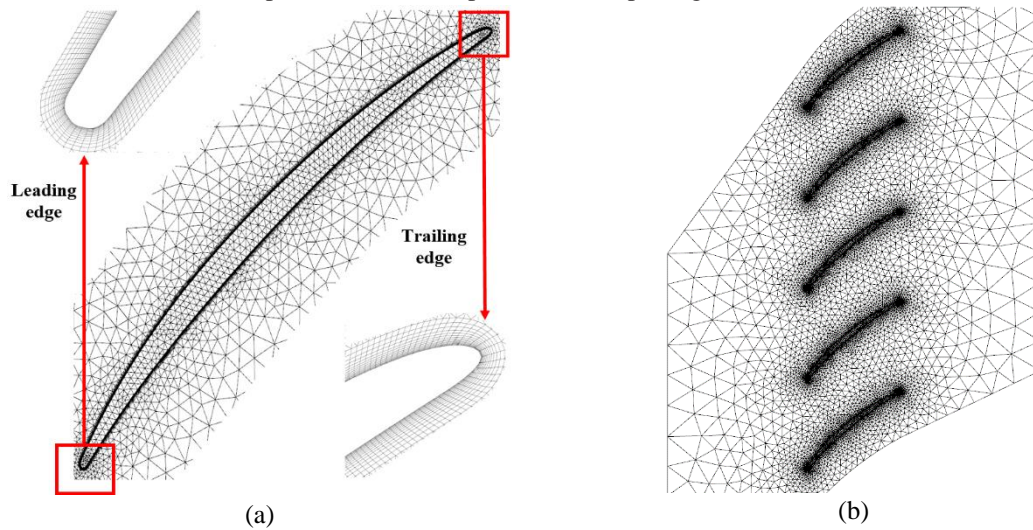


Figure 3: (a) Boundary-layer close to blade surface, (b) unstructured grid for the whole compressor cascade

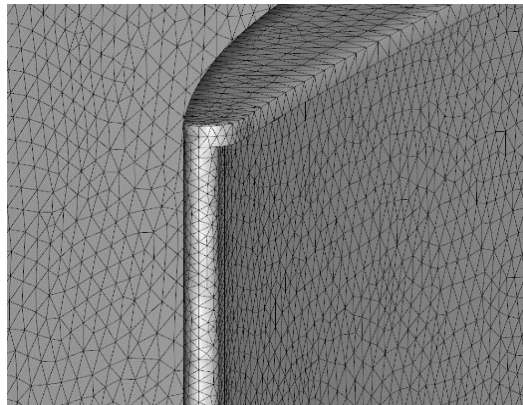


Figure 4: Close-up view of the mesh near the compressor blade with pressure side tip-winglet

A commercial CFD solver was used in the current numerical calculations to simulate the flow field in an axial compressor cascade with passive flow control method for tip-leakage flow. Reynolds-Averaged Navier-Stokes (RANS) equations were discretized using a Least Squares Cell Based, Implicit Finite-Volume Method and solved at each cell's centroid within the computational domain. Semi Implicit Method for Pressure Linked Equations (SIMPLE) approach was selected for the pressure-velocity coupling by solving momentum and pressure-based continuity equations in a coupled method. Second-order upwind discretization scheme was selected for the special discretization of pressure, momentum and modified turbulent viscosity variables. Spalart-Allmars (S-A) was used as turbulence model and, the results are compared with the experimental data in terms of modelling the turbulent viscosity in the near wall region.

Results and Discussions

1. Contours of static pressure coefficient on the end-wall:

The distribution of the static pressure coefficient on the end-wall is calculated from the simulation results using the equation provided by Zhong et al[5] in their experimental study, as indicated below:

$$c_p = \frac{P_{local} - P_{inlet}}{\frac{1}{2} \rho V_{inlet}^2} \quad (1).$$



Where c_p is the dimensionless static pressure coefficient, P_{local} is the local static pressure on end-wall, N/m^2 , P_{inlet} is the static pressure at inlet in N/m^2 , ρ_{inlet} is the flow density at inlet in kg/m^3 and V_{inlet} is the flow velocity at inlet in m/s^2 .

The static pressure coefficient is calculated for both the baseline case (NW) and the controlled blades (PW) at 50% blade span. The results are compared with the measured data at two different values of tip clearance at $\tau = 1.0\% c$ and $\tau = 1.5\% c$. Figure 5 shows comparison between the present numerical results (left) and measured data (right) of the static pressure contours on the end-wall.

Figure 5 shows the comparison between the present numerical results (left) and measured data (right) of the static pressure contours on the end-wall.

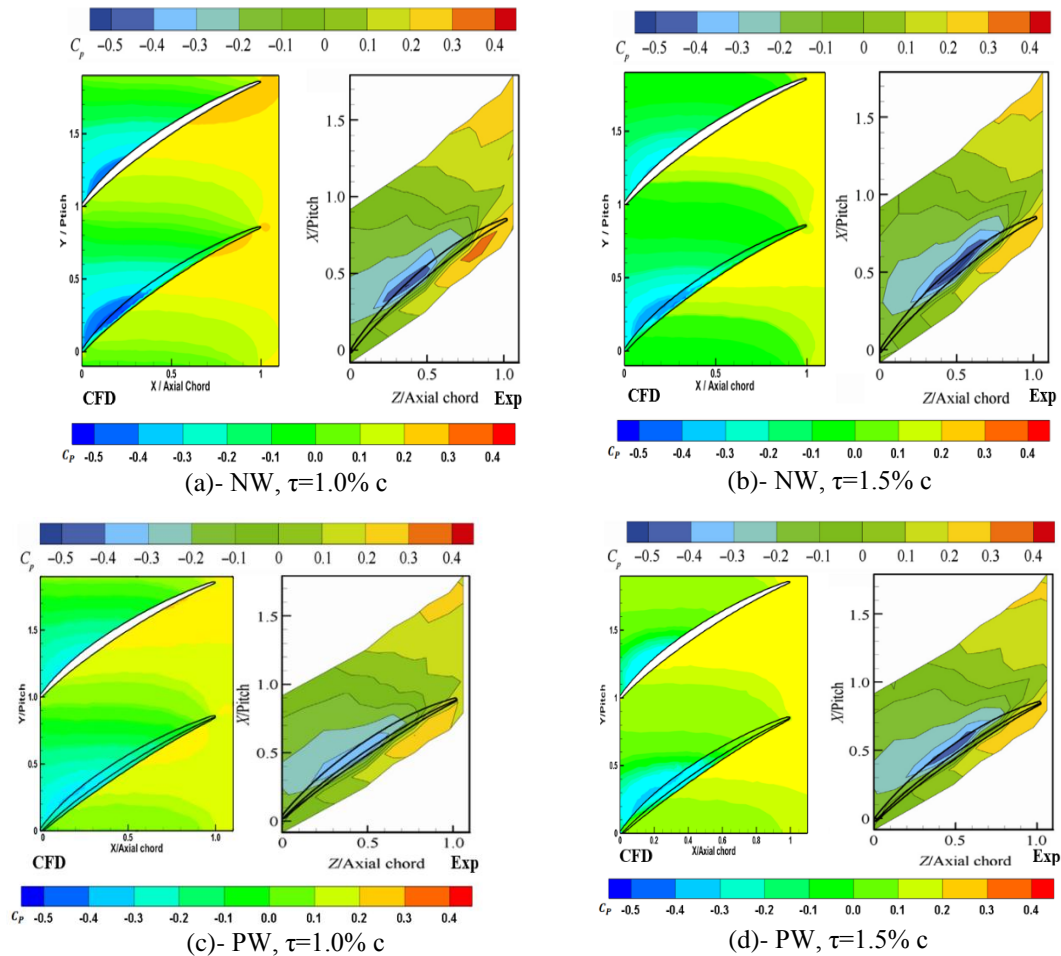


Figure 5: Comparison between the experimental and numerical results of static pressure coefficient at the end-wall

The plots show that the CFD model predicted accurately the existence of low-pressure region on the blade end-wall (suction side), however there is a little shifted for this region towards the blade leading edge although it has almost the same size. This low-pressure region for the baseline cases (a & b) is created due to the generation of the tip leakage vortex that moves downstream, hence the region moves downstream towards the blade trailing edge with increasing the tip gap.

On the other side, for the pressure-side winglet (cases c & d) as shown in Figure 8, the tip leakage vortex moved to suction side of the blade and mixed with the separation in the suction-side intensely.

2. The overall mass-averaged total pressure loss coefficient of the exit plane.

The overall mass-averaged total pressure loss coefficient of the exit plane (ω) was used to show the effectiveness of using tip winglet and which is defined as follows:



$$\omega = \frac{\int_{h/2}^h \int_0^t \rho W \omega dx dy}{\int_{h/2}^h \int_0^t \rho W dx dy} \quad (2).$$

Where h is the blade span, t the blade pitch, W axial-wise velocity.

Figure 6 shows the comparison numerical and experimental results for the overall total loss pressure variation in exit plane.

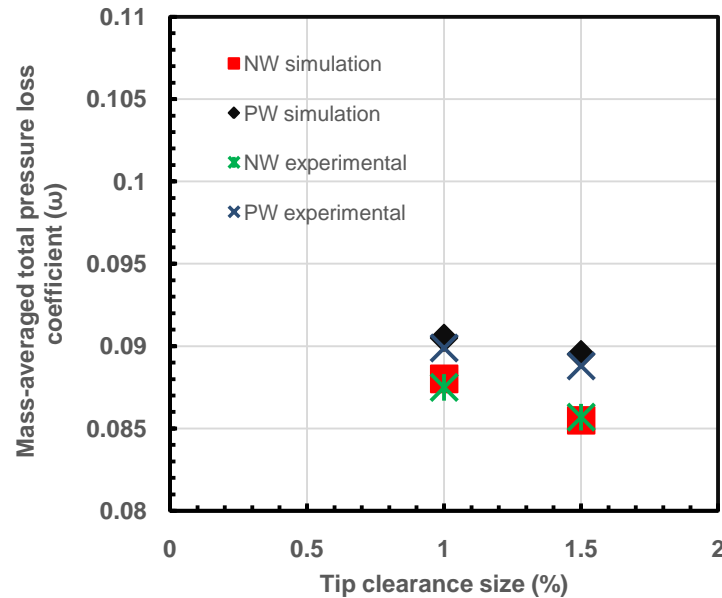


Figure 6: Comparison of measured and numerical exit mass-averaged total pressure loss coefficient.

The plot indicates for pressure-side winglet (PW), the overall mass-averaged total pressure loss coefficients are increased by 2.84% and 4.678% for tip clearance sizes of 1.0% and 1.5% of blade chord, so using pressure-side winglet increased the total pressure losses at the exit plane.

Conclusions

The effectiveness of applying a pressure tip-winglet design as passive flow control method of tip leakage flow loss in a highly loaded compressor cascade was investigated numerically. The numerical results were presented at two values of tip clearance of 1.0% c and 1.5% c and these results were compared with the available experimental data for both baseline (NW) and controlled blades (PW). The comparisons were carried out in terms of mass-averaged total pressure loss coefficient, static pressure coefficient on the end-wall. It was found that aerodynamics performance of the compressor cascade was deteriorated by using the pressure-side winglet design cause the strength of tip leakage vortex at the two studied values of tip clearance was increased compared to the baseline blade because the mass flow rate leakage through the tip gap was increased.

References

- [1]. C. Freeman, "Effect of tip clearance flow on compressor stability and engine performance," *Von Karman Institute for Fluid Dynamics Lecture Series*, vol. 5, 1985.
- [2]. J. A. Storer and N. A. Cumpsty, "Tip leakage flow in axial compressors," *ASME J. Turbomach*, vol. 113, pp. 252-259, 1991.
- [3]. S. Kang and C. Hirsch, "Numerical simulation of three-dimensional viscous flow in a linear compressor cascade with tip clearance," *Journal of turbomachinery*, vol. 118, pp. 492-502, 1996.
- [4]. A. Shavalikul and C. Camci, "A comparative analysis of pressure side extensions for tip leakage control in axial turbines," *ASME Paper No. GT2008-50782*, 2008.
- [5]. J. Zhong, S. Han, H. Lu, and X. Kan, "Effect of tip geometry and tip clearance on aerodynamic performance of a linear compressor cascade," *Chinese Journal of Aeronautics*, vol. 26, pp. 583-593, 2013.



- [6]. H. Shaobing and Z. Jingjun, "The influences of pressure-side winglet on aerodynamic performance of compressor cascade at different incidences," in *Consumer Electronics, Communications and Networks (CECNet), 2011 International Conference on*, 2011, pp. 5398-5401.
- [7]. J. Zhong, S. Han, and P. Sun, "The influence of suction-side winglet on tip leakage flow in compressor cascade," in *ASME 2011 Turbo Expo: Turbine Technical Conference and Exposition*, 2011, pp. 263-273.

